Asian Journal of Chemistry; Vol. 25, No. 18 (2013), 10460-10464

ASIAN JOURNAL OF CHEMISTRY

http://dx.doi.org/10.14233/ajchem.2013.15709

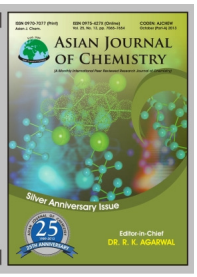

Synthesis and Characterization of D-A-D Type Chromophore DSeBT

JUNFENG TONG[1] and LILI AN[2,*]

[1]Key Laboratory of Optoelectronic Technology and Intelligent Control of Ministry Education, Lanzhou Jiaotong University, Lanzhou 730070, P.R. China
[2]School of Chemical Engineering, Northwest University for Nationalities, Lanzhou 730030, P.R. China

*Corresponding author: Fax: +86 931 4512928; Tel: +86 931 4516533; E-mail: anlili2011@163.com

(*Received*: 1 May 2013; *Accepted*: 20 November 2013) AJC-14427

A donor-acceptor-donor (D-A-D) type crystallization near infrared (NIR) absorbing chromophore **DSeBT** with a band gap of 0.84 eV is synthesized *via* palladium-catalyzed Stille coupling reaction. In thin film, the absorption region of **DSeBT** is from 300 and 1459 nm with the absorption peaks located at 380 and 1028 nm, while its photoluminescence peak in chloroform solution is observed at 1210 nm. The HOMO and LUMO energy levels of **DSeBT** are estimated at -4.86 and -4.02 eV, respectively. Furthermore, the thermal results reveal that **DSeBT** has a good thermal stability with decomposition temperature over 320 ºC and a very sharp crystallization peak at 174 ºC during the cooling run.

Key Words: Chromophore, Crystallization, Near infrared, Narrow band gap, Synthesis.

INTRODUCTION

Over the past few years, numerous efforts have been devoted to narrow band gap (NBG) organic materials with energy gap (E_g) lower than 2.0 eV owing to the promising applications of them in the organic photovoltaic solar cells (PSCs)[1,2], organic photodetectors[3,4] and near infrared light-emitting diodes (LEDs)[5,6]. Most importantly, some narrow band gap organic materials have been used as photosensitizers photodynamic therapy in the treatment of cancer[7]. Thus far, many narrow band gap organic materials have been witnessed [8-10]. Especially, narrow band gap conjugated polymers used in high performance photovoltaic solar cells and photodetectors have been extensively studied[11,12]. However, the performance of optoelectronic devices based on conjugated polymers are strongly related with the polymer molecular weight, polydispersion index and work-up procedure[13,14].

Compared with conjugated polymers (CPs), narrow band gap organic chromophores have well-defined molecular structure, definite molecular weight and high purity without batch-to-batch variations[15-17]. He *et al.*[18] reported a star-shaped molecule S(TPA-BT) with good solubility based on benzo[*c*][1,2,5]thiadizaole (BT) moiety, which showed the absorption edge of 667 nm and power conversion efficiency (PCE) of 1.3 % in photovoltaic solar cells[18]. Henson *et al.*[19] reported a series of D-A-D-A-D type chromophores based on asymmetric pyridal[2,1,3]thiadiazole (PT) unit, exhibiting that the absorption edge could reach 820 nm due to the fruitful electron density of the terminal donor. Qian *et al.*[20] reported a series of near infrared organic chromophores with the band gap of 1.19-0.56 eV based on benzo[1,2-*c*:4,5-*c*′]bis([1,2,5]-thiadiazole) (BBT) and its selenium analogues, which exhibited the exclusive near infrared emission of light-emitting diodes above 1000 nm. Interestingly, a liquid-crystal chromophore LC-BBT with band gap of 1.06 eV was reported by Li *et al.*[21] Moreover, the LC-BBT possessed columnar mesophase in aggregation state that was beneficial to the performance in photovoltaic device due to the increase of charge mobility[22,23]. Accordingly, the crystallization near infrared chromophores should be potential promising materials for exploiting tandem solar cell with high performance, near infrared liquid crystal display and near infrared photodetector.

In this paper, we design and synthesize a D-A-D type near infrared crystal chromophore **DSeBT** (Fig. 1). **DSeBT** with optical band gap of 0.85 eV is soluble in common organic solvents and easily fabricated into thin film by spin-coating. The absorption peaks of **DSeBT** in thin film are located at 380 and 1028 nm, while photoluminescence peak in solution is observed at 1210 nm. Its thermal result reveals good thermal stabilities with decomposition temperature of 325 ºC.

EXPERIMENTAL

^{1}H and ^{13}C NMR spectra are recorded on a Bruker DRX 400 spectrometer operating, respectively at 400 MHz (for ^{1}H)

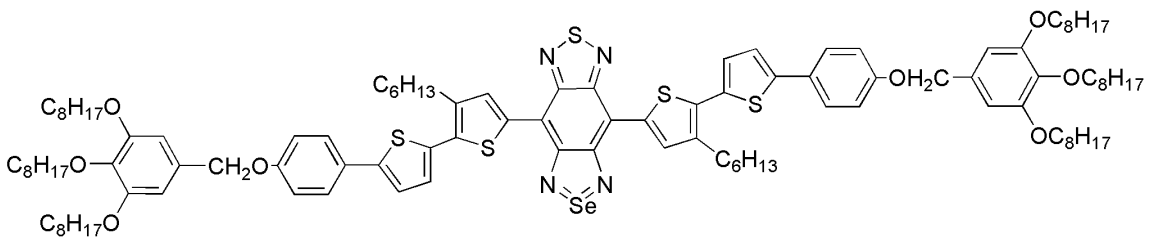

Fig. 1. Structure of synthesized chromophore **DSeBT**

and 100 MHz (for ^{13}C) in $CDCl_3$ with chemical shifts in δ units (ppm) relative to internal standard tetramethylsilane (TMS). GC-MS and fast atom bombardment mass spectrometry (FAB-MS) are obtained on GC-MS (TRANCE2000, Fiunigan Co. FAB-MS (VG ZAB-HS). Thermogravimetric (TG) analysis is conducted on a TGA 2050 (TA instruments) thermal analysis system under a heating rate of 20 ºC min^{-1} and a nitrogen flow rate of 20 mL min^{-1}. Differential scanning calorimetry (DSC) measurement is running on a DSC 204 F1 (NETZSCH) thermal analysis system and the sample is heated from 30 to 200 ºC at a rate of 5 ºC min^{-1} under continuous nitrogen flow. Elemental analyses are performed on a Vario EL Elemental Analysis Instrument (Elementar Co.). UV-VISIBLE near infrared absorption spectra is recorded on a Lambda 900 Perkin-Elmer spectrophotometer. Cyclic voltammogram (CV) is recorded on a CHI660 (Shanghai Chenhua Co.) electrochemical workstation with platinum electrodes and a silver pseudo-reference electrode in nitrogen saturated acetonitrile solution of 0.1 M tetra-*n*-butylammonium hexafluorophosphate (Bu_4NPF_6). The photoluminence (PL) spectra are collected using the PTI fluorescence instrument.

The manipulations involving air-sensitive reagents are performed under a dry argon atmosphere. All reagents are obtained from Aldrich, Acros and TCI Chemical Co. Some solvents are carefully dried and purified under argon flow. Compounds 4,7-dibromobenzo[*c*][1,2,5]thiadiazole (**1**)[26], 4,7-dibromo-5,6-dinitrobenzo[*c*][1,2,5]thiadiazole (**2**)[27], 4,7-di(4-hexylthien-2-yl)-5,6-diaminobenzo[*c*][1,2,5]- thiadiazole (**4**)[22], 4,7-bis(4-hexylthien-2-yl)-5,6-dinitrobenzo[*c*][1,2,5]-thiadiazole (**3**)[28], 4,8-bis(4-hexylthien-2-yl)[1,2,5]-selenadiazolo[3,4-*f*]benzo[*c*][1,2,5]thiadiazole (**5**)[20], 4,8-bis(5-bromo-4-hexylthien-2-yl)[1,2,5]selenadiazolo[3,4-*f*]benzo[*c*][1,2,5]thiadiazole (**6**)[20], 2-{4-(3,4,5-tri(octyloxy)-benzyloxy)phenyl}-5-tri(butyl)stanylthiophene (**7**)[21] are synthesized according to the corresponding procedures.

Synthesis

4,8-Bis(4-hexylthien-2-yl)[1,2,5]selenadiazolo[3,4-*f*]-benzo[*c*][1,2,5]thiadiazole (**5**). To a solution of 4,7-bis(4-hexylthien-2-yl)-5,6-diaminobenzo[*c*][1,2,5]thiadiazole **4** (2.49 g, 5 mmol) in the mixture of THF and ethanol (1:4 in volume) at 60 ºC under argon flow, selenium dioxide (2.2 g, 20 mmol) in ethanol was added to dropwise and the reaction was kept at 60 ºC for 4 h. After cooling to ambient temperature, the mixture was poured into water and extracted with chloroform. The solvent was removed under reduced pressure. The residue was purified by chromatography, giving the product as green powder (2.01 g, Yield, 70 %). ^1H NMR (400 MHz, $CDCl_3$), δ (ppm): 7.73 (s, 2H), 7.14 (dd, 2H), 2.68 (m, 4H), 1.70 (m, 4H), 1.25-1.56 (m, 12H), 0.9 (t, 6H); FAB-MS: 574; Anal. calcd. (%) for $C_{26}H_{30}N_4S_3Se$: C, 55.43; H, 5.27; N, 9.77, S, 16.77, Se, 13.76; Found (%): C, 55.42, H, 5.30, N, 9.76. S, 16.8.

4,8-Bis(5-bromo-4-hexylthien-2-yl)[1,2,5]selenadiazolo-[3,4-*f*]benzo[*c*][1,2,5]thiadiazole (6): *N*-Bromosuccinimide (NBS) (1.96 g, 11 mmol) was added slowly into a solution of compound **5** (2.87 g, 5 mmol) in 120 mL THF at ambient temperature and the reaction was stirred overnight under dark. Then the mixture was poured into water and extracted with chloroform. The combined organic phase was dried by anhydrous Na_2SO_4 and evaporated under reduced pressure to remove the solvent. The residue was purified by chromatography, giving the product as dark green powder (2.56 g, yield, 70 %). ^1H NMR (400 MHz, $CDCl_3$), δ (ppm): 7.73 (s, 2H), 2.68, (m, 4H), 1.70 (m, 4H), 1.25-1.56 (m, 12H), 0.9 (t, 6H); FAB-MS: 732; Anal. calcd. (%) for $C_{26}H_{28}N_4Br_2S_3Se$: C, 42.69, H, 3.86, Br, 21.85, N, 7.66, S, 13.15, Se, 10.79; Found (%): C, 42.67, H, 3.90, N, 7.65, S, 12.3.

Compound DSeBT[21]: To a solution of 2-{4-(3,4,5-tris-(octyloxy)benzyloxy)phenyl}-5-tri(butyl)stanylthiophene **7** (4.69 g, 4.7 mmol) and 4,8-bis(5-bromo-4-hexylthien-2-yl)[1,2,5]selenadiazolo[3,4-*f*]benzo[*c*][1,2,5]thiadiazole **6** (1.46 g, 2 mmol) in anhydrous THF, $Pd(PPh_3)_2Cl_2$ (2 mol %) was added. The mixture was refluxed under argon for 24 h. After removal of the solvent under reduced pressure, the residue was purified by column chromatography. The solid was dissolved in a small amount of THF and then precipitated from methanol twice to give a brown dark solid (3.18 g, yield, 85 %). ^1H NMR (400 MHz, $CDCl_3$), δ (ppm): 8.85 (s, 2H), 7.59 (d, 4H), 7.31-7.24 (m, 4H), 7.03 (d, 4H), 6.66 (s, 4H), 5.00 (s, 4H), 3.99 (m, 12H), 2.94 (br, 4H), 1.85-1.76 (m, 24H), 1.50-1.31 (m, 64H), 0.9 (t, 24H); ^{13}C NMR (100 MHz, $CDCl_3$), δ (ppm): 156.60, 153.37, 144.25, 140.27, 138.08, 136.51, 135.26, 131.33, 127.22, 126.88, 122.73, 115.31, 114.92, 106.19, 73.46, 70.56, 69.18, 31.93, 31.86, 30.37, 29.89, 29.58, 29.44, 29.40, 29.32, 26.14, 22.78, 22.69, 14.20, 14.11; FAB-MS: 1871.9. Anal. calcd. (%) for $C_{108}H_{150}N_4O_8S_5Se$: C, 69.31, H, 8.08, N, 2.99, S, 8.57 Se, 4.22; Found: C, 69.20; H, 8.00, N, 3.10, S, 8.45.

RESULTS AND DISCUSSION

Synthesis and characterization: The synthetic strategy for **DSeBT** is illustrated in **Scheme-I**. Compounds **5**, **6** and **7** are prepared for the published procedures[20,21]. **DSeBT** is synthesized from compound **6** and **7** *via* Stille-coupling reaction. The chemical structure of the **DSeBT** is verified by ^1H NMR, ^{13}C NMR, FAB-MS and elemental analysis. The characteristic peaks at 6.66-8.85 ppm can be assigned to the resonance of

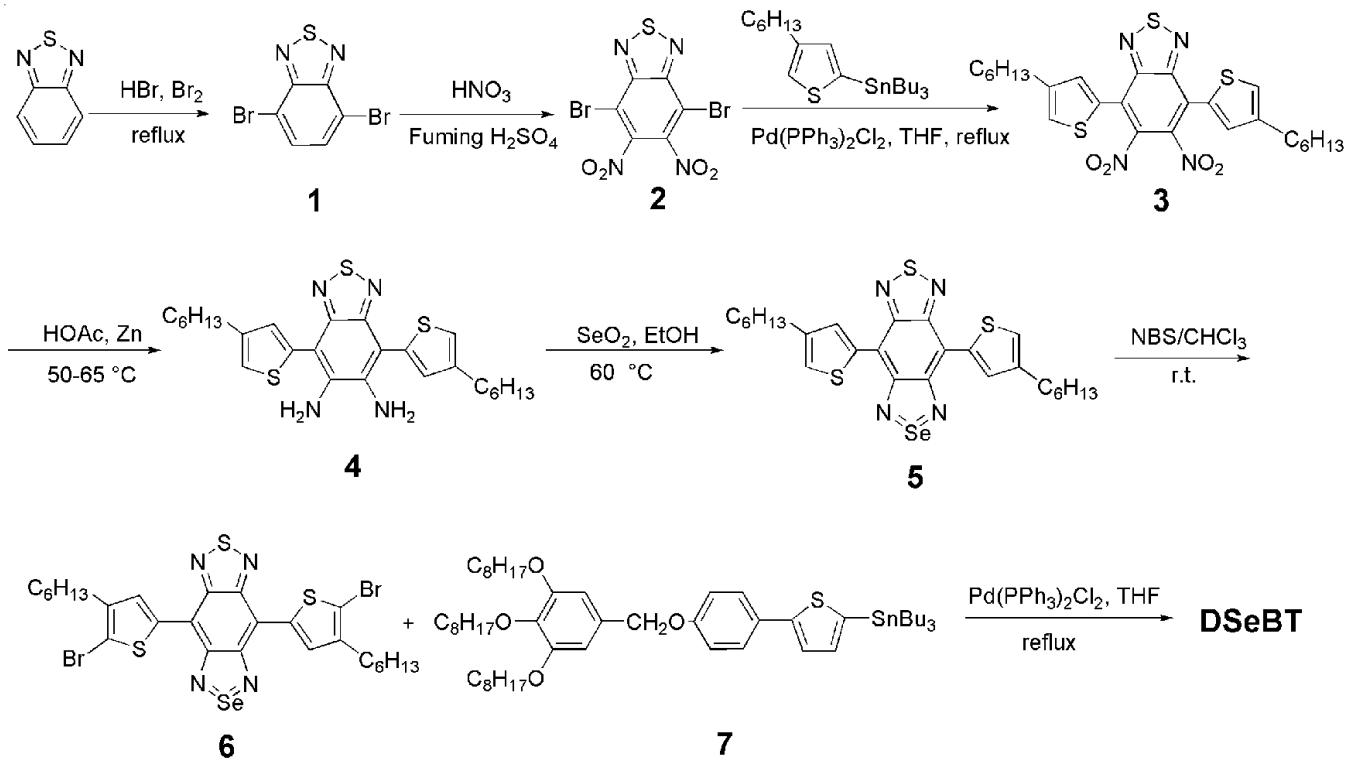

Scheme-1: Synthesis of chromophoroe **DSeBT**

protons on the thiophene rings and phenylene rings of the **DSeBT** (Fig. 2). The peaks in the range of 3.99-5.00 ppm arise from the protons of methylene (-CH_2O-, -OCH_2R). The peaks in the range of 0.9-2.94 ppm arise from the protons of alky substituents. Furthermore, both FAB-MS and elemental analysis results are also in good agreement with the molecular structure of **DSeBT**.

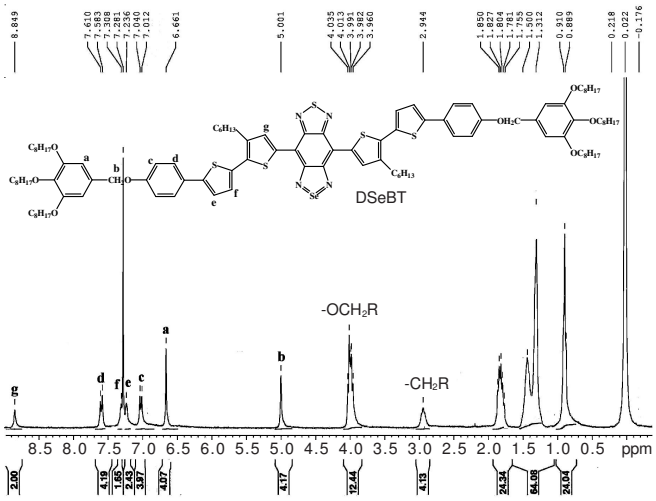

Fig. 2. ^{1}H NMR spectrum of **DSeBT**

Thermal properties: The thermal stability of **DSeBT** is investigated by thermogravimetric analysis (Fig. 3a). TGA digram reveals that **DSeBT** has a good thermal stability with decomposition temperature (T_d, 5 % weight loss) of 325 ºC. The thermal phase transition for **DSeBT** is analyzed by DSC (Fig. 3b). As evidenced by the appearance of a very sharp crystallization peak at 174 ºC during the cooling run, it suggests

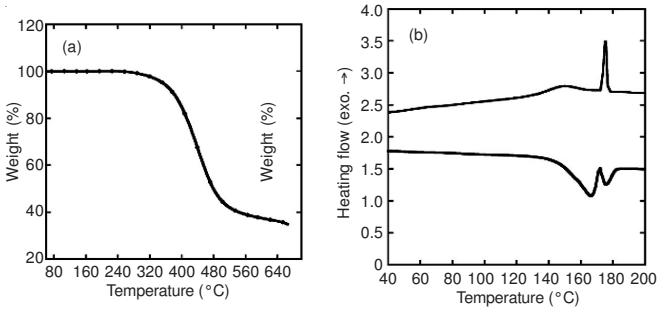

Fig. 3. TGA (a) thermograph and DSC (b) curves for **DSeBT** in nitrogen at scans of 20 and 5 ºC min^{-1}, respectively

isotropic to liquid crystal phase around 174 ºC and another from liquid crystal phase to another phase around 152 ºC. In the heating process, two transitions occur at 166 and 173 ºC. All data indicate **DSeBT** is a crystallization chromophore[21].

Optical properties: The normalized absorption spectra of **DSeBT** in dilute $CHCl_3$ solution and thin film are shown in Fig. 4. The related optical information is summarized in Table-1. The absorption spectra of **DSeBT** in dilute solution display two peaks at 382 and 960 nm. The absorption peak (382 nm) is attributed to the π-π* and n-π* transitions of the molecule, while the other peak (960 nm) placed in near infrared region is assigned to the intramolecular chare transfer transition between the peripheral electron-donor unit and central strong electron-withdrawing core. In comparison with the solution, corresponding absorption peaks are shifted to around 380 and 1028 nm in thin film, respectively. The absorbtion band in 600-1500 nm region is well-separated from higher energy bands, indicating a stronger charge transfer character for D-A-D chromophore[29]. Fig. 4 also shows 68 nm red-shift in the longer wavelength region comparing that in dilute chloroform

TABLE-1
OPTICAL AND ELECTROCHEMICAL PROPERTIES OF **DSeBT**

Molecule	Absorption spectra				PL spectra		Cyclic voltammetry		
	Solution	Film			Solution	Film	*p*-Doping $E_{on}^{ox}/_{HOMO}$	*n*-Doping $E_{on}^{red}/_{LUMO}$	E_g^{elec}
	λ_{max}(nm)	λ_{max}(nm)	λ_{onset}(nm)	E_g^{opt}(eV)	λ_{max}(nm)	λ_{max}(nm)	(V)/(eV)	(V)/(eV)	(eV)
DSeBT	382, 960	380,1028	1459	0.85	1210	–	0.46/-4.86	-0.38/-4.02	0.84

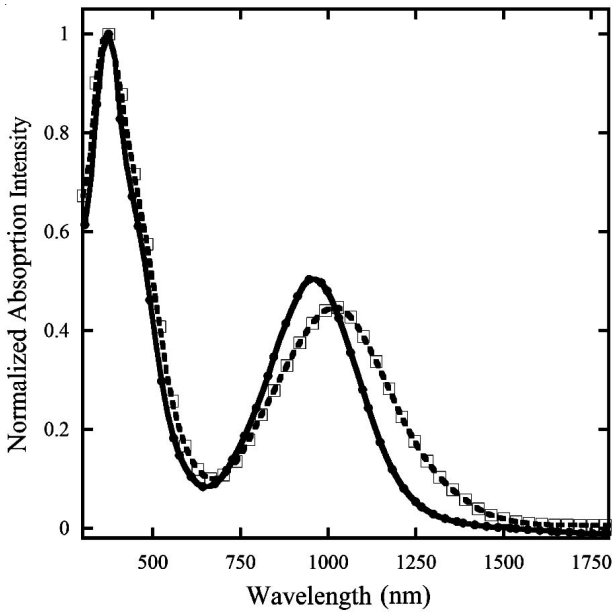

Fig. 4. Normalized absorption spectra of **DSeBT** in $CHCl_3$ solution (solid line) and solid thin film (dotted line)

solution, which is larger than that of LC-BBT (60 nm)[21]. Since the onset band wavelength of **DSeBT** in thin film is 1459 nm, the corresponding optical band gap (E_g = 1240/λ_{onset} eV) is estimated, namely 0.85 eV. As shown in Fig. 5, the photoluminescence emission peak of the **DSeBT** in $CHCl_3$ solution at 1210 nm. And the stokes shift is 250 nm, which is larger than that for LC-BBT (224 nm)[21]. However, the photoluminescence of intrinsic thin film of **DSeBT** is not monitored, probably due to the heavy atom quenching effect of selenium (heavy selenium atom may increase the intersystem crossing from singlet to triplet)[24,25] or the non-radiative probability of $S_1 \rightarrow S_0$ increase as decreasing the width of energy gaps of $S_0 \rightarrow S_1$[30].

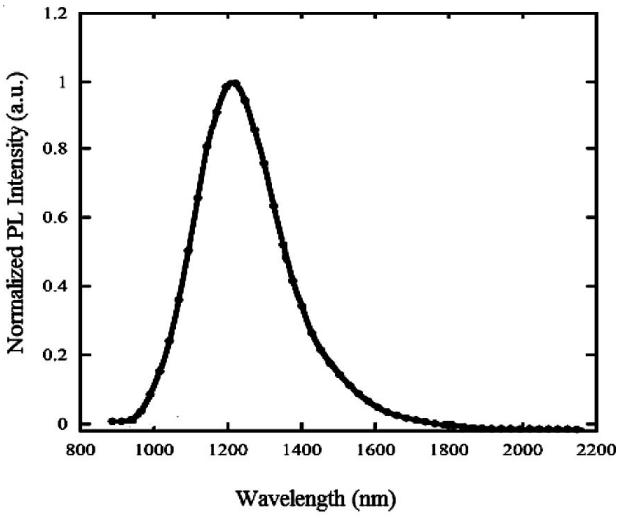

Fig. 5. Normalized photoluminescence spectrum of **DSeBT** in diluted $CHCl_3$ solution (λ_{ex} = 780 nm)

Electrochemical properties: In order to investigate the electrochemical behaviours such as charge transport propertites and assess the ionization potentials and electrochemical stability of **DSeBT**, the electrochemical measurement has been performed on the thin film for **DSeBT** (Fig. 6). The related data are listed in Table-1. The reduction potential (E_{red}) is at around -0.38 V, while the oxidation potential (E_{ox}) is around 0.46 eV. And the HOMO and LUMO energy levels of the **DSeBT** calculated by empirical formulas (E_{HOMO} = -e(E_{ox} + 4.4) (eV) and E_{LOMO} = -e(E_{red} + 4.4) (eV))[31] are -4.86 and -4.02 eV, respectively. And the electrochemical band gap (E_g^{elec} = E_{LOMO} – E_{HOMO}) is 0.84 eV, coinciding with the optical band gap (E_g^{opt}= 0.85 eV)[21].

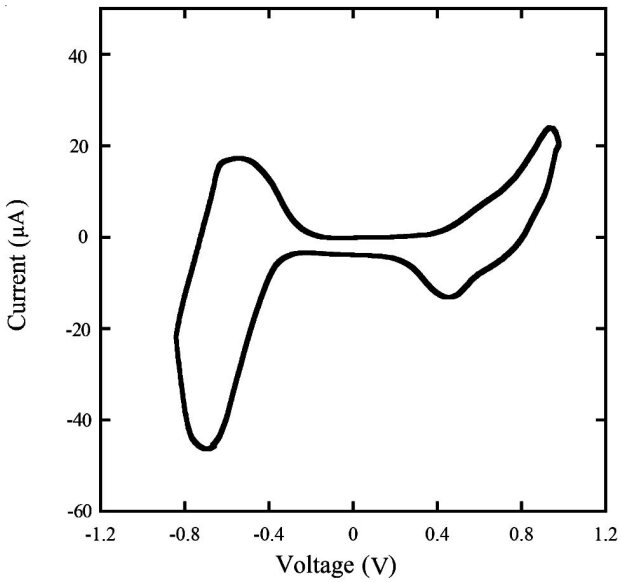

Fig. 6. Cyclic voltammogram for **DSeBT** in 0.1 mol L^{-1} acetonitrile solution of Bu_4NPF_6

Conclusion

A narrow band gap chromophore **DSeBT** possessing good solubility in common organic solvents and easily manufactured into thin film by spin-coating has been designed and synthesized. The chemical structure, electrochemical, optical properties are characterized and investigated by NMR, UV-VISIBLE near infrared absorption spectrometry, photoluminescence spectrometry, cyclic voltammetry and TGA and DSC measurement *etc*. The absorbtion region of **DSeBT** achieves 300-1457 nm with elelctrochemical band gap of 0.84 eV, while photoluminescence peak of the chromophore in $CHCl_3$ solution is around 1210 nm with a Stokes shift of 250 nm. The thermal results reveal that **DSeBT** has good thermal stability with decomposition temperature over 320 ºC and a very sharp crystallization peak at 174 ºC during the cooling run. Moreover, HOMO and LUMO energy levels are at -4.86 and -4.02 eV, respectively.

These primary results suggest that **DSeBT** should be a potential promising material for exploiting high performance tandem solar cells and near infrared photodetectors.

ACKNOWLEDGEMENTS

The authors are deeply grateful to the Young Scholars Science Foundation of Lanzhou Jiaotong University (No. 2011038).

REFERENCES

1. J.Y. Kim, K. Lee, N.E. Coates, D. Moses, T.-Q. Nguyen, M. Dante and A.J. Heeger, *Science*, **317**, 222 (2007).
2. J. Hou, Z. Tan, Y. Yan, Y. He, C. Yang and Y. Li, *J. Am. Chem. Soc*., **128**, 4911 (2006).
3. Y. Yao, Y. Liang, W. Shhrotriya, S. Xiao, L. Yu and Y. Yang, *Adv. Mater.*, **19**, 3979 (2007).
4. G. Qian, J. Qi, J.A. Davey, J.S. Wright and Z.Y. Wang, *Chem. Mater.*, **24**, 2364 (2012).
5. G. Qian, Z. Zhong, M. Luo, D. Yu, Z. Zhang, Z.Y. Wang and D. Ma, *Adv. Mater.*, **21**, 111 (2009).
6. Y. Yang, R.T. Farley, T.T. Steckler, S.-H. Eom, J.R. Reynolds, K.S. Schanze and J. Xue, *Appl. Phys. Lett.*, **93**, 163305 (2008).
7. A. Yuan, J. Wu, X. Tang, L. Zhao, F. Xu and Y. Hu, *J. Pharm. Sci.*, **102**, 6 (2013).
8. T.-Y. Chu, J. Lu, S. Beaupré, Y. Zhang, J.-R. Pouliot, S. Wakim, J. Zhou, M. Leclerc, Z. Li, J. Ding and Y. Tao, *J. Am. Chem. Soc.*, **133**, 4250 (2011).
9. L. Dou, J. You, J. Yang, C.-C. Chen, Y. He, S. Murase, T. Moriarty, K. Emery, G. Li and Y. Yang, *Nat. Mater.*, **6**, 180 (2012).
10. Y. Xia, L. Wang, X. Deng, D. Li, X. Zhu and Y. Cao, *Appl. Phys. Lett.*, **89**, 081106 (2006).
11. H.-Y. Chen, J. Hou, S. Zhang, Y. Liang, G. Yang, Y. Yang, L. Yu, Y. Wu and G. Li, *Nat. Photonics*, **3**, 649 (2009).
12. X. Gong, M. Tong, Y. Xia, W. Cai, J.S. Moom, Y. Cao, G. Yu, C.-L. Shieh, B. Nilsson and A.J. Heeger, *Science*, **325**, 1665 (2009).
13. Y. Yao, J. Hou, Z. Xu, G. Li and Y. Yang, *Adv. Funct. Mater*., **18**, 1783 (2008).
14. J. Peet, N.S. Cho, S.K. Lee and G.C. Bazan, *Macromolecules*, **41**, 8655 (2008).
15. G.C. Welch, L.A. Perez, C.V. Hoven, Y. Zhang, X.-D. Dang, A. Sharenko, M.F. Toney, E.J. Kramer, T.-Q. Nguyena and G.C. Bazan, *J. Mater. Chem.*, **21**, 12700 (2011).
16. M.T. Lloyd, J.E. Anthony and G.G. Malliaras, *Mater. Today*, **10**, 34 (2007).
17. B. Walker, C. Kim and T.-Q. Nguyen, *Chem. Mater.*, **23**, 470 (2011).
18. C. He, Q. He, Y. Yi, G. Wu, F. Bai, Z. Shuai and Y. Li, *J. Mater. Chem.*, **18**, 4085 (2008).
19. Z.B. Henson, G.C. Welch, T. van der Poll and G.C. Bazan, *J. Am. Chem. Soc.*, **134**, 3766 (2012).
20. G. Qian, B. Dai, M. Luo, D. Yu, J. Zhan, Z. Zhang, D. Ma and Z.Y. Wang, *Chem. Mater*., **20**, 6208 (2008).
21. X. Li, A. Liu, S. Xun, W. Qiao, X. Wan and Z.Y. Wang, *Org. Lett*., **10**, 3785 (2008).
22. I.H. Stapff, V. Stumpflen, J.H. Wendorff, D.B. Spohn and D. Mobius, *Liq. Cryst.*, **23**, 613 (1997).
23. P. Herwig, C.W. Kayser, K. Müllen and H.W. Spiess, *Adv. Mater*., **8**, 510 (1996).
24. R. Yang, R. Tian, Q. Hou, W. Yang and Y. Cao, *Macromolecules*, **36**, 7453 (2003).
25. R. Yang, R. Tian, Q. Hou, Y. Zhang, Y. Li, W. Yang, C. Zhang and Y. Cao, *J. Polym. Sci. Part A: Polym. Chem*., **43**, 823 (2005).
26. K. Pilgram, M. Zupan and R. Skile, *J. Heterocycl. Chem*., **7**, 629 (1970).
27. T. Uno, K. Takagi and M. Tomoeda, *Chem. Pharm. Bull.*, **28**, 1909 (1980).
28. Y. Xia, X. Deng, L. Wang, X. Li, X. Zhu and Y. Cao, *Macromol. Rapid Commun*., **27**, 1260 (2006).
29. S. Amthor, C. Lambert, S. Dümmler, I. Fischer and J. Schelter, *J. Phys. Chem. A*, **110**, 5204 (2006).
30. J.R. Lakowicz, Principles of Fluorescence Spectroscopy, Kluwer, New York (1999).
31. D.M. de Leeuw, M.M.J. Simenon, A.R. Brown and R.E.F. Einerhand, *Synth. Met.*, **87**, 53 (1997).